Surface Hardening of Ni-base Alloys with Boronizing Technique†

Fukuhisa MATSUDA*, Kazuhiro NAKATA** and Yasuhiro NISHIO***

Abstract

Boronizing of commercial Ni-base heat-resistant alloys as Inconel 600, Inconel 625, Inconel 713C, Udiment 500 and Hastelloy B, has been investigated by means of a furnace heat treatment burrying in amorphous boron powder under an argon atmosphere at 1223 K and 10.8 Ks. The hardnesses of the boronized surface on the above alloys showed the range of Hv 1000 to 1600 depending on chemical compositions.

Moreover, in order to investigate the effect of each alloying element in pure Ni on increase in boronized surface hardness, various Ni-binary alloys, which contained Ti, Zr, Hf, V, Nb, Ta, Cr, Mo, Mn, Fe, Co, Al or Si elements up to 30%, were boronized. The boronized surface of the alloys has been investigated from metallographic and X-ray analyses and hardness distribution. Finally hardness estimation of boronized surface of commercial Ni-base alloys has been tried using the experimental results of hardenability of Ni-binary alloys.

KEY WORDS: (Surface Hardening) (Boronizing) (Ni-base Alloy) (Ni-binary Alloy)

1. Introduction

Recently nickel and nickel-base alloys have been widely used in various industrial plants and equipments. However as surface hardness of these metal and alloys is not so hard, abrasive and wearing resistances are not satisfied for engineering uses.

Therefore surface hardening of Ni and Ni-base alloys is required from many fields as heat-resistant, incorrodile, non-magnetic and low temperature industries. The authors have tried to investigate the hardenability of commercially used Ni-base alloys by means of boronizing technique in comparison with hardenability of Ni metal which was reported by the authors[1].

As a result, it was cleared that the hardenability of Ni-base alloy was differentiated depending on alloy compositions in Ni.

Therefore, in order to make clear the effect of alloying element in Ni on hardenability for boronizing, various Ni-binary alloys were made and boronized. Then metallurgical and analytical investigations were done for these boronized surface layers. Moreover from these results an equation which can estimate the surface hardness after boronizing was investigated, when chemical compositions are known in Ni-alloys.

2. Experimental Procedure

2.1 Materials used

Materials used in this experiment are commercial used Ni-base alloys of Inconel 600, 625, 713C, Udimet 500 and Hastelloy B as shown in **Table 1** and experimental Ni-binary alloys of Ni-Ti, -Zr, -Hf, -V, -Nb, -Ta, -Cr, -Mo, -Mn, -Fe, -Co, -Al, -Si, as shown in **Table 2**. Experimental Ni-binary alloys were melted in an argon furnace with RF

Table 1 Chemical compositions of commercial Ni-base alloys used.

	Alloy	Nominal composition (wt%)
Ni base Alloys	Inconel 600	Ni-15.8Cr,7.2Fe,0.2Si
	Inconel 625	Ni-22Cr,9Mo,4Nb,3Fe,0.3Si,0.2Ti,0.2Al
	Inconel 713C	Ni-12.5Cr,6.1Al,4.2Mo,2.5Fe,2Nb,0.8Ti,0.1Zr
	Udimet 500	Ni-19Cr,18Co,4Fe,4Mo,2.9Ti,2.9Al
	Hastelloy B	Ni-28Mo,5Fe,2.5Co,0.6Cr,0.3V

Table 2 Chemical compositions of experimental Ni-binary alloys used.

Alloy System	Composition (wt%)
Ni - Ti	Ti : 1, 1.5, 4, 7
- Zr	Zr : 1
- Hf	Hf : 1
- V	V : 1, 5, 10, 15
- Nb	Nb : 1, 5, 10
- Ta	Ta : 1, 3, 5, 10
- Cr	Cr : 5, 10, 20, 30
- Mo	Mo : 5, 10, 20
- Mn	Mn : 10, 30
- Fe	Fe : 10, 20
- Co	Co : 20
- Al	Al : 6
- Si	Si : 5

† Received on May 6, 1987

* Professor
** Research Associate
*** Co-operative Researcher, Professor of KINKI University

Transactions of JWRI is published by Welding Research Institute of Osaka University, Ibaraki, Osaka 567, Japan

and after that forged and annealed with 1023 K × 1.8 Ks. Specimen size for boronizing was 5 × 15 mm square and 3 mm in thickness, and was boronized after polishing with #1500 emery paper and removal of grease.

2.2 Boronizing technique

Using amorphous solid boron powder the specimen was packed in a carbon crucible and heated in a furnace purged with argon gas flow. The detailed treatment technique has been reported in literatures[1−2]. Heating temperature for boronizing treatment was 1223 K and holding time was 10.8 Ks.

After boronizing treatment the specimen was rinsed in acetone reagent with ultrasonic generator.

2.3 Investigations

After boronizing the specimens were investigated metallographic microstructures and analyses of boronized surface layer in crosssection with OM and SEM with EDX.

The hardness measurements in crosssection was done by a micro Vickers hardness tester with a quadrangular pyramid with 0.25 N (25 gf) load.

X-ray analysis was also done for determination of boride layers on specimen surface.

3. Experimental Results and Discussions

3.1 Commercial Ni-base alloys

3.1.1 Features and morphology of boronizing layer

Boronized crosssection for Ni and commercial Ni-base alloys are shown in **Fig. 1 (a)** to **(f)**. Boronized layer in Ni metal in (a) was composed of only one layer of a dense "compound layer", under which there is no special boride in both of boundary and inside of grain. The compound layer shows about 40μm in depth. Some porosities were seen at boundary between the compound layer and base Ni metal. In Inconel 600 in (b) boronized layer was composed of three different parts, the dense "compound layer" at the top, precipitation part of boride for whole grain called "dispersed layer" at the second and precipitation part of boride particles along grain boundary called "grain boundary precipitation zone" at the bottom. The depths of the above three parts from the top surface were about 25, 50 and 100μm, respectively. In Inconel 625 in (c) boronized layer was composed of three parts, although precipitations along grain boundary were much clear compared with Inconel 600. The depths of the three parts are about 25, 40 and 80μm, respectively. In Inconel 713C in (d) boronized layer was composed of two parts, "compound layer" and "dispersed layer". There is no "grain boundary precipitation zone", and the precipitates is fine needle-like shaped in "dispersed layer". The depths

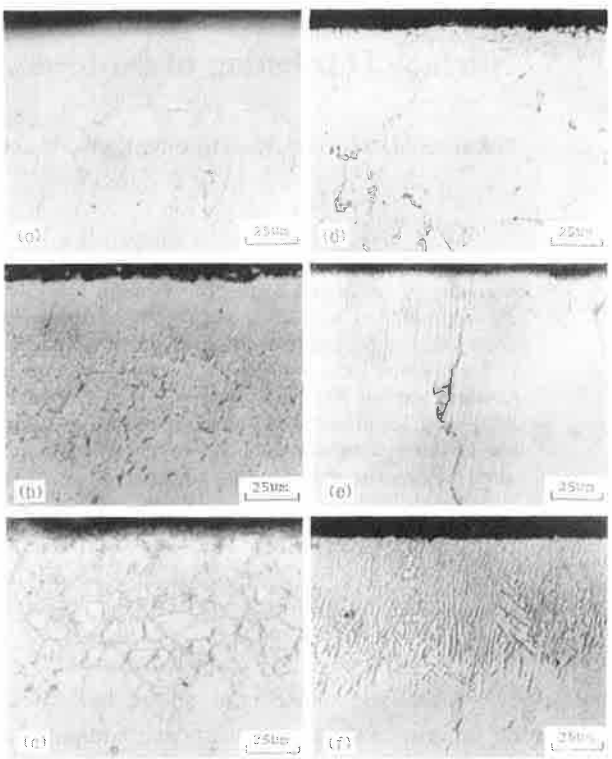

Fig. 1 Crosssectional microstructures of boronized commercial Ni-base alloys (1223K–10.8Ks) (×400); (a) pure Ni, (b) Inconel 600, (c) Inconel 625, (d) Inconel 713C, (e) Udimet 500, (f) Hastelloy B

were about 20 and 40μm, respectively.

Boronized layers of Udimet 500 in (e) were similar those of Inconel 713C, whose depth was about 20 and 40μm, respectively. In Hastelloy B in (f) boronized layer was also composed of two parts, that is, "compound layer" and "dispersed layer" whose depth was about 20 and 60μm, respectively. There are obvious needle-like shaped precipitates in "dispersed layer".

Figure 2 shows a general illustration of boronized layer of Ni-base alloys which was obtained from Fig. 1 (a) to (f). The authors called hereafter three parts as briefly (A) layer for "compound layer", (B) layer for "dispersed layer" and (C) zone for "grain boundary precipitation zone".

Next, chemical analyses of borized layer were done with EDX for Inconel 600. The results showed in **Fig. 3 (a)** and **(b)**. In (A) layer Ni and Fe were lowered compar-

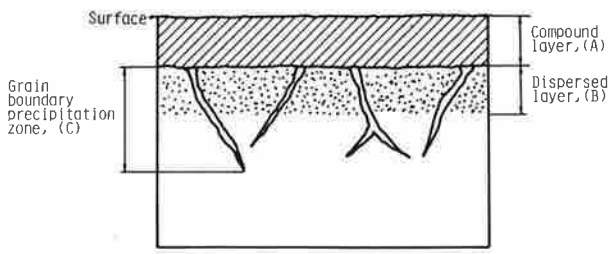

Fig. 2 General illustration of boronized layers and zone in commercial Ni-base alloys.

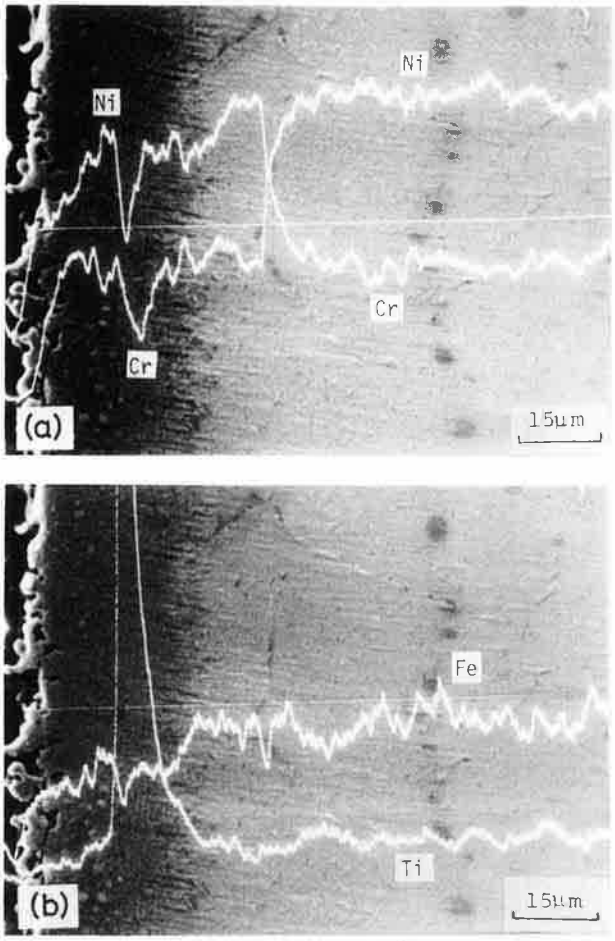

Fig. 3 EDX analyses of Ni, Cr, Fe and Ti elements of boronized layer of Inconel 600; (a) Ni, Cr, (b) Fe, Ti

ing those of base metal, Cr was no obvious change in both, but Ti was locally increased where Cr and Ni were obviously decreased. As a result, it is considered that some complex borides containing Ni, Cr, Fe and Ti are formed in (A) layer.

3.1.2 Hardness of boronizing layer

Hardness distributions of boronized Ni, Inconel 600, 625, 713C, Udimet 500 and Hastelloy B in crosssection were shown in **Fig. 4** which represented the distance from the specimen surface in horizontal axis. Upper the figure the thicknesses of various layer and zone, that is (A), (B) and (C), are shown for each alloy. For Ni metal only (A) layer whose hardness showed about Hv 800 was formed for about 40μm. The hardest hardness was obtained in case of Inconel 625 of all as Hv 1580 and order of the maximum hardness was Udimet 500 and Hastelloy B of about Hv 1300, in Inconel 600 of Hv 1100 and in Inconel 713C of Hv 1040. The maximum hardness was kept within the range of (A) layer and then the hardness was promptly decreased to that of base metal in (B) layer and there was no hardness change in (C) zone. In comparison with boronized Ni metal each Ni-base alloy showed higher hardness in its boronized (A) layer. This was a reason that

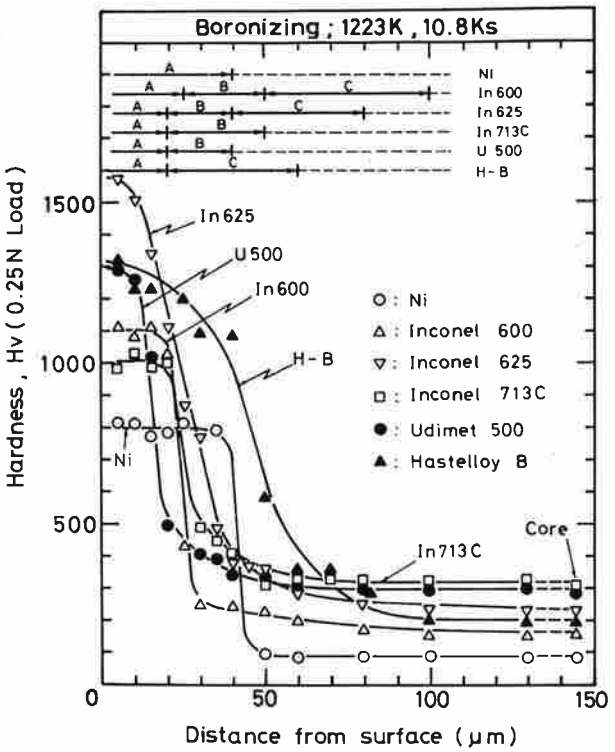

Fig. 4 Hardness distributions of boronized pure Ni and commercial Ni-base alloys (1223K–10.8Ks).

Cr, Fe, Ti and other alloying elements were contained as mixture in the boronized layer of Ni-base alloy. Judging from both the maximum hardness and the depth of hardened zone Inconel 625 and Hastelloy B are anticipated to be useful alloy for boronizing Ni-base alloy.

3.2 Experimental Ni-binary alloys

3.2.1 Effect of individual alloying element on boronizing characteristics

Effect of alloying element on the features of boronizing layer of Ni was described in the following according as metal group of the Periodic Table of Elements after treated of 1223K and 10.8 Ks.

(1) IVa group (Ti, Zr, Hf)

Hardness distributions of Ni-Ti alloy specimens after boronizing were shown in **Fig. 5** in which that of Ni metal was inserted in a broken line. Type and depth of boronized layer were also illustrated in the upper of the figure. The type of boronized layer of Ni-Ti alloys was single (A) layer whose hardness kept a constant, that is Hv 950 for 1 Ti, 1000 for 1.5 Ti, 1100 for 4 Ti and 1500 for 7 Ti alloys. The depth of boronized layer was 30 to 40μm for all Ni-Ti alloys. In **Fig. 6** crosssectional boronized structures were shown as (a) for 1.5 Ti (X400), (b) for 4 Ti (X400) and (c) for 7 Ti (X1000 in SEM). The boronized layer of 1.5 Ti as well as 1 Ti showed single (A) layer in which two different types of boride were precipitated as spotty state. The boronized layer of 4 Ti showed

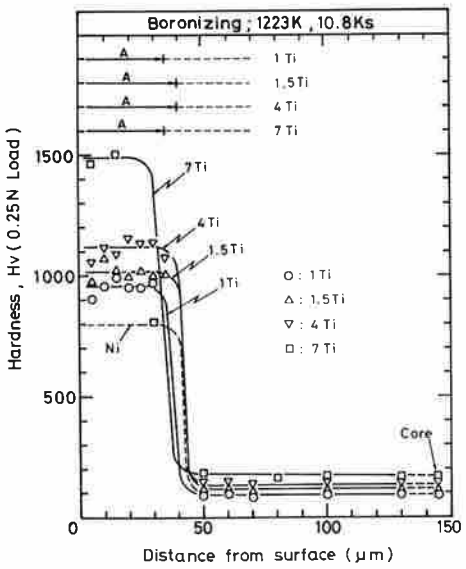

Fig. 5 Hardness distributions of boronized Ni-Ti alloys.

single (A) layer under which (B) layer was seen a little. Moreover that of 7 Ti showed (A) and (B) layers.

Hardness distributions of Ni-1 Zr and - 1 Hf alloy specimens after boronizing were shown in **Fig. 7**. The boronized layers were single (A) layer whose depth was 30 and 50μm, respectively. The hardness of boronized layer was elevated to about Hv 1000 for both alloys. **Figure 8** showed the crosssectional microstructures of 1 Zr for (a) (X400) and 1 Hf for (b) (X400). Both boronized layers showed single (A) layer, though the surface of 1 Hf was considerably rough.

(2) Va group (V, Nb, Ta)

Hardness distributions and feature of boronized layer of Ni-V alloy specimens were shown in **Fig. 9**. Alloying of 1 V increased the hardness to Hv 1000 and an increase of alloying element to 10 to 15 V increased the hardness to Hv 1400. The boronized layer consisted of (A) layer and (C) zone for 1 and 5 V, single (A) for 10 V and (A) and (B) for 15 V in which depth of (A) layer was 45, 45, 40 and 25μm, respectively. In **Fig. 10** crosssectional microstructures of 1, 5, 10 and 15 V after boronizing were shown for (a) to (d), respectively. Needle-like boride layer was seen in (A) layer for all Ni-V alloys. (C) zone in 5 V and (B) layer in 15 V alloy reached to 150 and 100μm in depth, respectively.

Hardness distributions and feature of boronized layer of Ni-Nb alloy specimens were shown in **Fig. 11**. Alloying of Nb up to 5% reached the hardness to Hv 950, and widened the boronized (A) layer to 50 to 60μm. However alloying of 10 Nb increased the hardness to Hv 1300 and narrowed (A) layer to 35μm. **Figure 12** showed crosssectional microstructures of 1, 5 and 10 Nb for (a) to (c) in X400, respectively. There were some voids in boundary of (A) layer and base metal in 1 and 5 Nb boronized

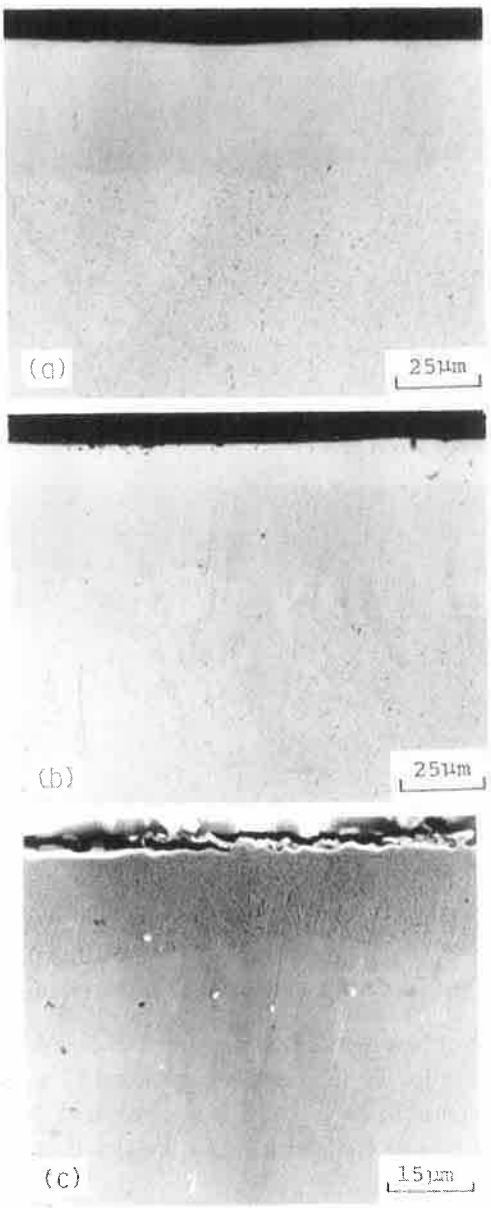

Fig. 6 Crosssectional microstructures of boronized Ni-Ti alloys; (a) 1.5 Ti alloy (X400), (b) 4 Ti alloy (X400), (c) 7 Ti alloy (X1000, SEM)

alloys. (C) zone was a little seen in 5 Nb alloy. In 10 Nb alloy (A) layer was narrowed and made double layers in it.

Figure 13 showed hardness distributions and features of boronized Ni-Ta alloys. The hardness distributions of 1, 3 and 5 Ta alloys were almost the same as Hv 1100, but that of 10 Ta was lowered as Hv 900 and was narrower than the other alloys. Increasing Ta up to 5% increased the depth of (B) layer, although (A) layer was almost the same as 40μm. Crosssectional microstructures of boronized Ni-Ta alloys were shown in **Fig. 14 (a)** to **(d)** in X400. There was no voids in boundary zone between boronized area and base metal.

(3) VIa group (Cr, Mo)

Figure 15 showed hardness distributions and features

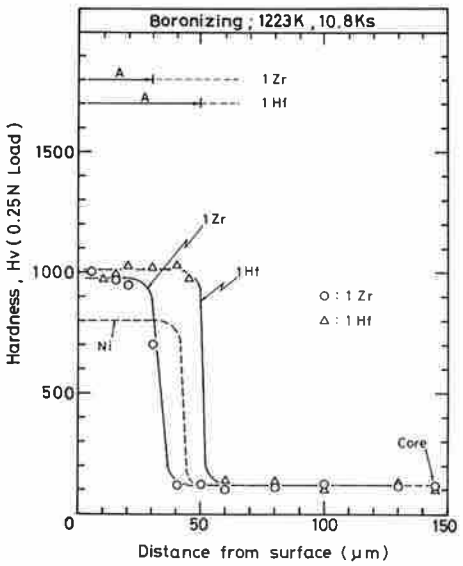

Fig. 7 Hardness distributions of boronized Ni-1 Zr and -1 Hf alloys.

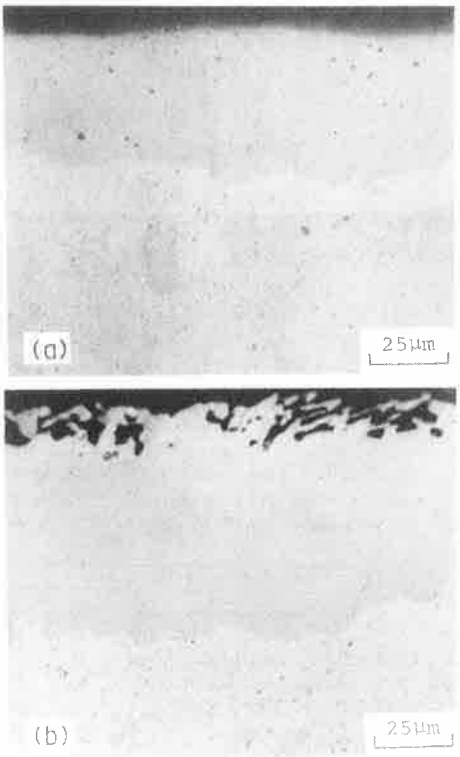

Fig. 8 Crosssectional microstructures of boronized Ni-1 Zr and -1 Hf alloys (×400); (a) 1 Zr alloy, (b) 1 Hf alloy

of boronized Ni-Cr alloys. The boronized zone was composed of (A) and (C), and partly (B) layer in which the thickness of (A) layer was 30 to 50μm. An increase in Cr content in boronized zone showed an increase in hardness in (A) layer. In 30 Cr the hardness reached to more than Hv 1500. Crosssectional microstructures of boronized Ni-Cr alloys were shown in **Fig. 16 (a)** to **(c)** in ×400. (C) zone in Ni-Cr alloys reached to about 100μm. Needle-like borides were seen in (A) layer of 10 and 30 Cr alloys. (B)

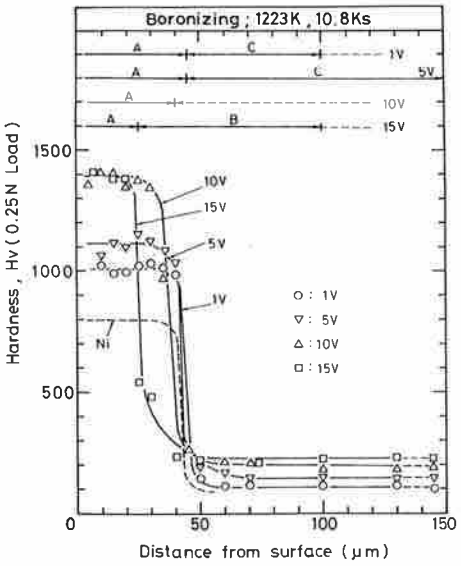

Fig. 9 Hardness distributions of boronized Ni-V alloys.

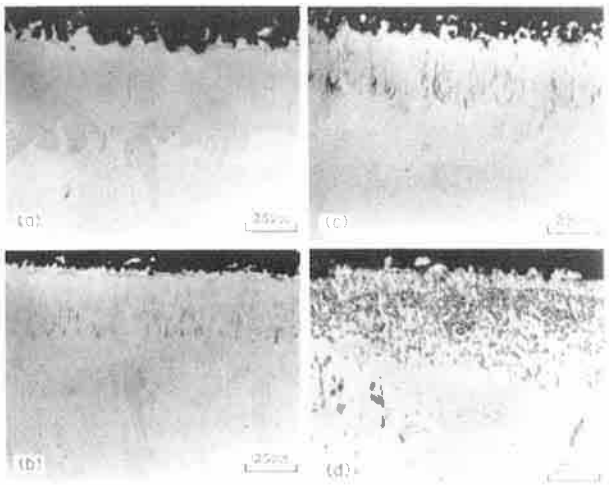

Fig. 10 Crosssectional microstructures of boronized Ni-V alloys (×400); (a) 1 V alloy, (b) 5 V alloy, (c) 10 V alloy, (d) 15 V alloy

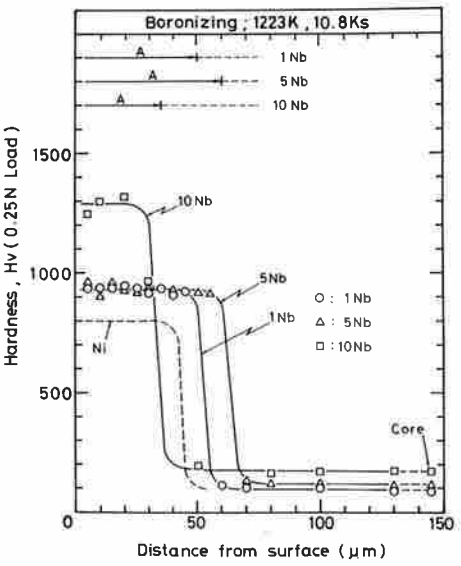

Fig. 11 Hardness distributions of boronized Ni-Nb alloys.

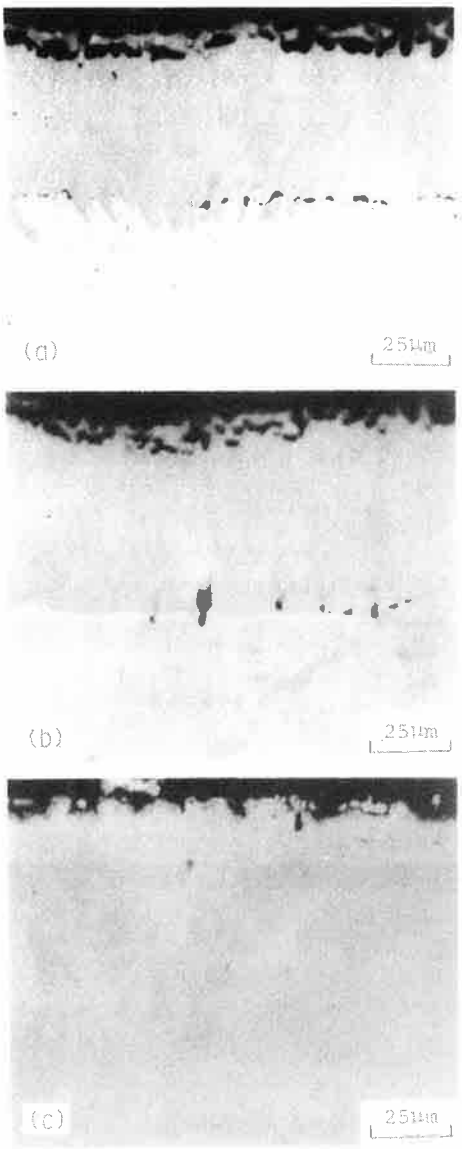

Fig. 12 Crosssectional microstructures of boronized Ni-Nb alloys (X400); (a) 1 Nb alloy, (b) 5 Nb alloy, (c) 10 Nb alloy

layer was clearly seen in 30 Cr alloy.

Figure 17 showed hardness distributions and features of boronized Ni-Mo alloys.

The boronized zone was composed of (A) layer and rarely (C) zone for 5 and 10 Mo, (A) and (B) layers for 20 Mo alloy. The thickness of (A) layer showed about 45μm for 5 and 10 Mo, and about 20μm for 20 Mo alloy. The hardness reached about Hv 1000-1100 for 5 and 10 Mo, and about Hv 1300 for 20 Mo alloy. Crosssectional microstructures of boronized Ni-Mo alloys were shown in **Fig. 18 (a)** to **(c)** in X400. Needle-like borides were precipitated in (B) layer (about 80μm) of 20 Mo alloy, although (A) layer was narrowed to about 20μm.

(4) VIIa group (Mn)

Figure 19 showed hardness distributions and features of boronized Ni-Mn alloys. The boronized zone was

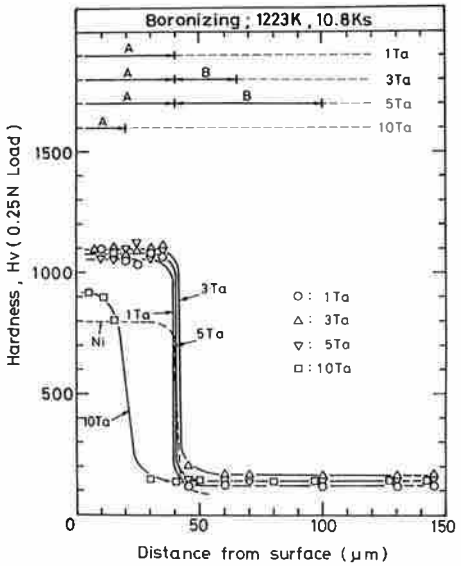

Fig. 13 Hardness distributions of boronized Ni-Ta alloys.

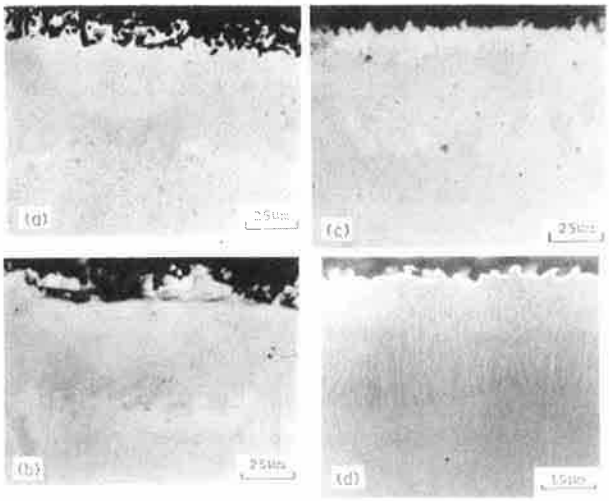

Fig. 14 Crosssectional microstructures of boronized Ni-Ta alloys (X400); (a) 1 Ta alloy, (b) 3 Ta alloy, (c) 5 Ta alloy, (d) 10 Ta alloy

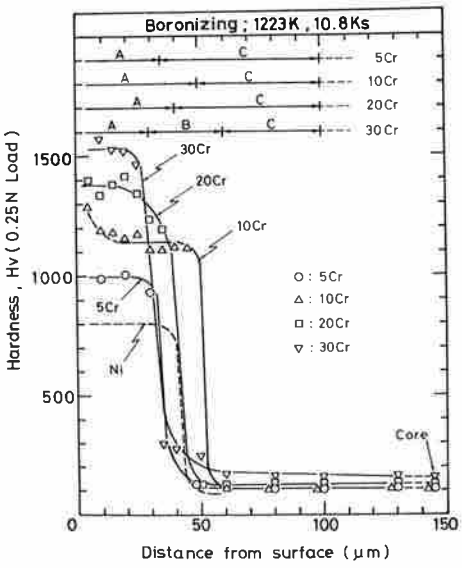

Fig. 15 Hardness distributions of boronized Ni-Cr alloys.

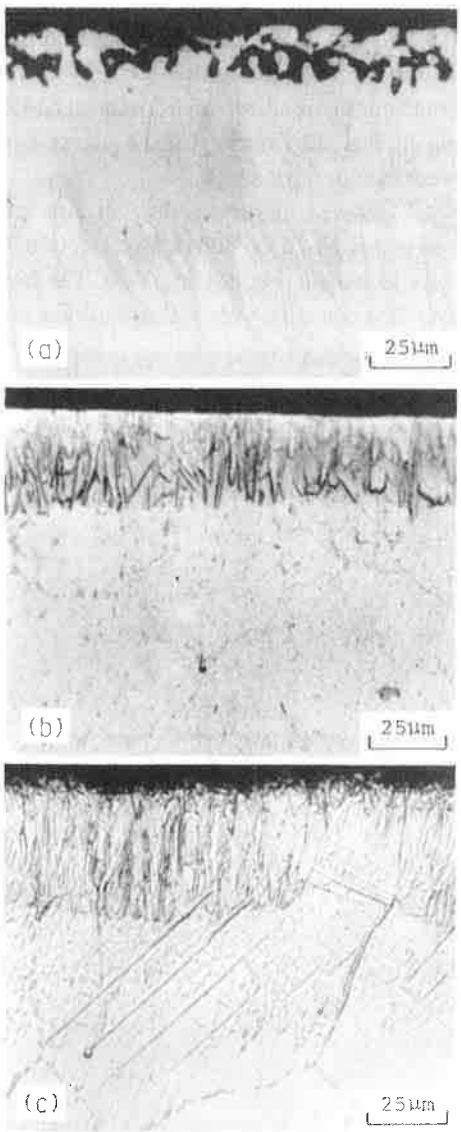

Fig. 16 Crosssectional microstructures of boronized Ni-Cr alloys (X400); (a) 5 Cr alloy, (b) 10 Cr alloy, (c) 30 Cr alloy

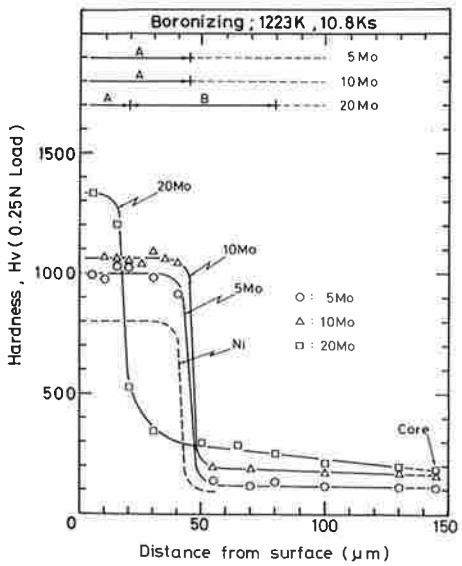

Fig. 17 Hardness distributions of boronized Ni-Mo alloys.

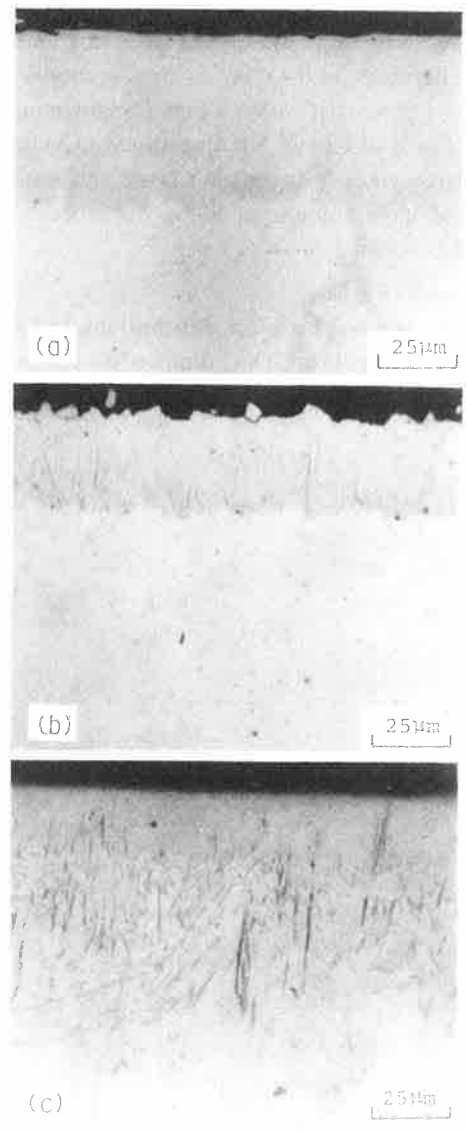

Fig. 18 Crosssectional microstructures of boronized Ni-Mo alloys (X400); (a) 5 Mo alloy, (b) 10 Mo alloy, (c) 20 Mo alloy

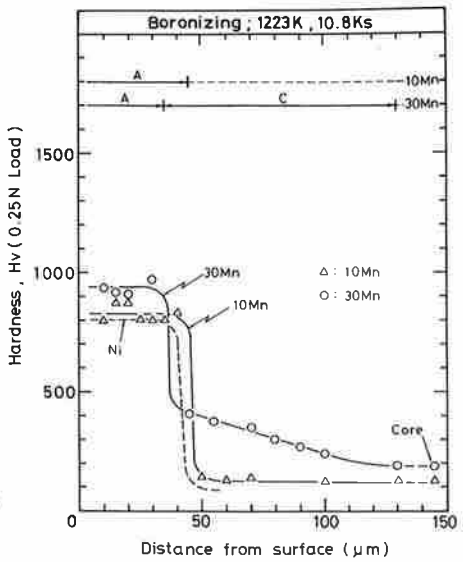

Fig. 19 Hardness distributions of boronized Ni-Mn alloys.

composed of single (A) for 10 Mn and (A) and (C) for 30 Mn alloy. The addition of Mn does not increase so much in hardness in (A) layer. Crosssectional microstructures of boronized Ni-Mn alloys are shown in **Fig. 20 (a)** and **(b)** in X400. In 30 Mn separation of (A) layer was seen by large voids between (A) layer and base alloy. Addition of large amount of Mn is not suitable for Ni alloy to be boronized.

(5) VIII group (Fe, Co)

Figure 21 showed hardness distributions and features of boronized Ni-Fe alloys. The boronized zone was mainly

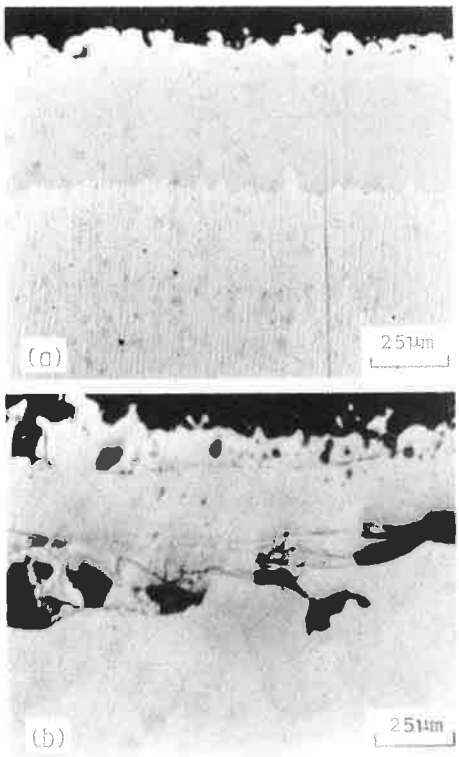

Fig. 20 Crosssectional microstructures of boronized Ni-Mn alloys (X400); (a) 10 Mn alloy, (b) 30 Mn alloy

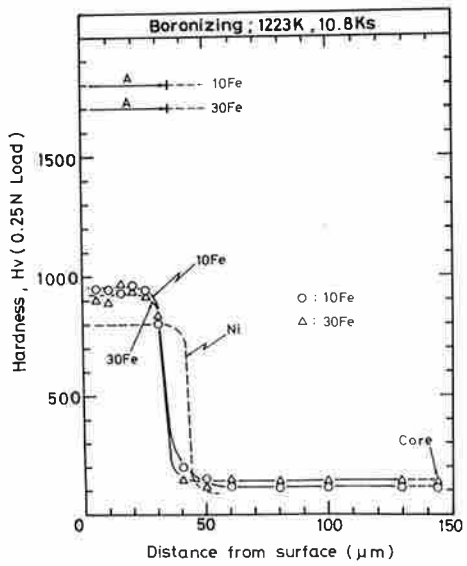

Fig. 21 Hardness distributions of boronized Ni-Fe alloys.

(A) layer and hardness was almost same Hv 900 to 1000 for both 10 and 30 Fe alloys. Addition of Fe in Ni was not so useful for increase in hardness by boronizing. Crosssectional microstructures of boronized Ni-Fe alloys were shown in **Fig. 22 (a)** and **(b)**. (A) layer and party (C) zone were seen in both alloys.

Figure 23 showed hardness distributions and features of boronized Ni-20 Co alloys. Crosssectional microstructure was shown in **Fig. 24** in X400. The boronized zone of (A) layer and (C) zone and hardness of about

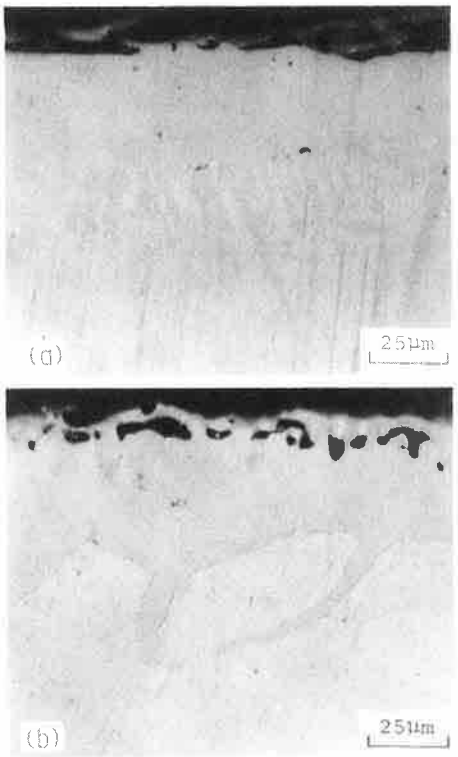

Fig. 22 Crosssectional microstructures of boronized Ni-Fe alloys (X400); (a) 10 Fe alloy, (b) 30 Fe alloy

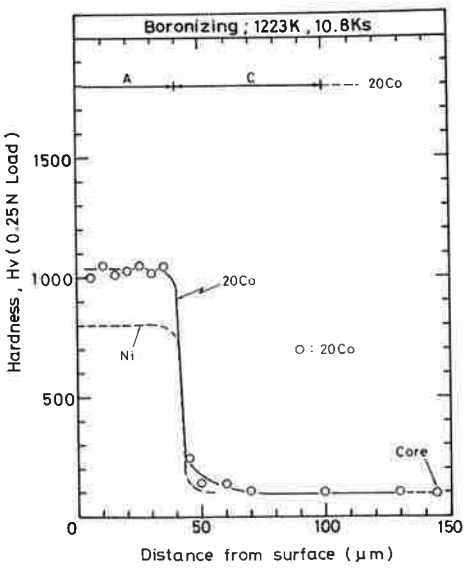

Fig. 23 Hardness distributions of boronized Ni-20 Co alloy.

Hv 1000 are formed.

(6) IIIb group (Al) and IVb group (Si)

Figure 25 showed hardness distributions and features of boronized Ni-6Al and Ni-5Si alloys. Addition of Al did not increase in hardness in boronized (A) layer of Ni, but that of Si increased a little.

Crosssectional microstructures were shown in **Fig. 26 (a)** and **(b)** ×400. The boronized zone is composed of (A) and partly (C) layer for 6 Al alloy, and (A) and (C) layers for 5 Si alloy.

3.2.2 Comparative evaluation for boronizing features of individual alloying element

(1) Comparison of hardenability

Table 3 collectively shows the maximum hardness and thickness of each layer in boronizing zone for commercial Ni-base and Ni-binary alloys after 1223K-10.8 Ks boronizing. Moreover, **Figure 27** shows the effect of individual alloying element on the maximum hardness of boronized Ni-binary alloys. Generally on increasing of each alloying element shows an increase in hardness of boronized layer.

Fig. 24 Crosssectional microstructures of boronized Ni-20 Co alloy (×400).

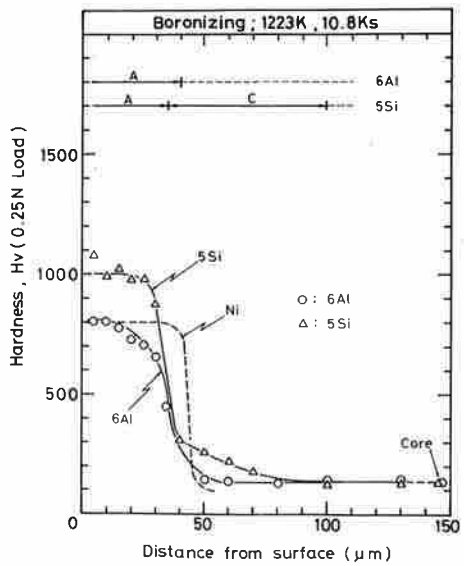

Fig. 25 Hardness distributions of boronized Ni-6 Al and Ni-5 Si alloys.

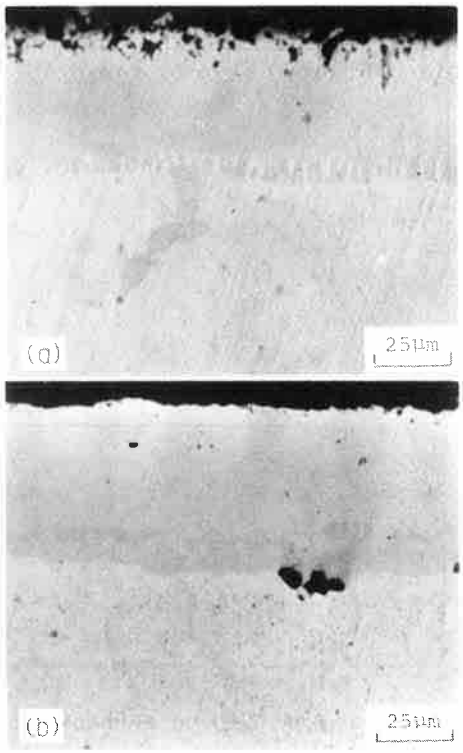

Fig. 26 Crosssectional microstructures of boronized Ni-Al and -Si alloys (×400); (a) 6 Al alloy, (b) 5 Si alloy

Table 3 Collective summary of maximum hardness and thicknesses of various boride layers and zone for Ni alloys used.

	Material	Hardness (Hv)		Thickness of boronized layer (μm)		
		Maximum	Base	A*1	B*2	C*3
Commercial alloy	Ni	800	85	40	-	-
	Inconel 600	1120	160	25	25	75
	Inconel 625	1580	230	20	20	60
	Inconel 713C	1030	300	20	30	-
	Udimet 500	1300	300	20	20	-
	Hastelloy B	1300	215	20	40	-
IVa	1Ti	1000	95	35	-	-
	1.5Ti	1050	100	40	-	-
	4Ti	1160	120	40	-	60
	7Ti	1500	170	35	-	-
	1Zr	1000	100	30	-	-
	1Hf	1050	90	50	-	-
Va	1V	1040	110	45	-	55
	5V	1150	150	45	-	105
	10V	1400	200	40	-	-
	15V	1400	215	20	80	-
	1Nb	950	90	50	-	-
	5Nb	960	120	60	-	40
	1Ta	1100	120	40	-	-
	3Ta	1100	160	40	25	-
	5Ta	1100	140	40	-	60
	10Ta	930	160	20	-	-
VIa	5Cr	1010	100	35	-	65
	10Cr	1300	130	40	-	60
	20Cr	1400	110	50	-	50
	30Cr	1580	150	30	30	70
	5Mo	1020	100	45	-	-
	10Mo	1100	160	45	-	-
	20Mo	1330	185	20	50	-
VIIa	10Mn	870	130	40	-	-
	30Mn	980	195	35	-	95
VIII	10Fe	960	110	35	-	-
	30Fe	970	150	35	-	-
	20Co	1080	100	40	-	60
IIIb	6Al	830	130	40	-	-
IVb	5Si	1050	130	35	-	65

*1 A:Compound layer of boride
*2 B:Dispersed layer of boride in matrix
*3 C:Grain boundary precipitation zone

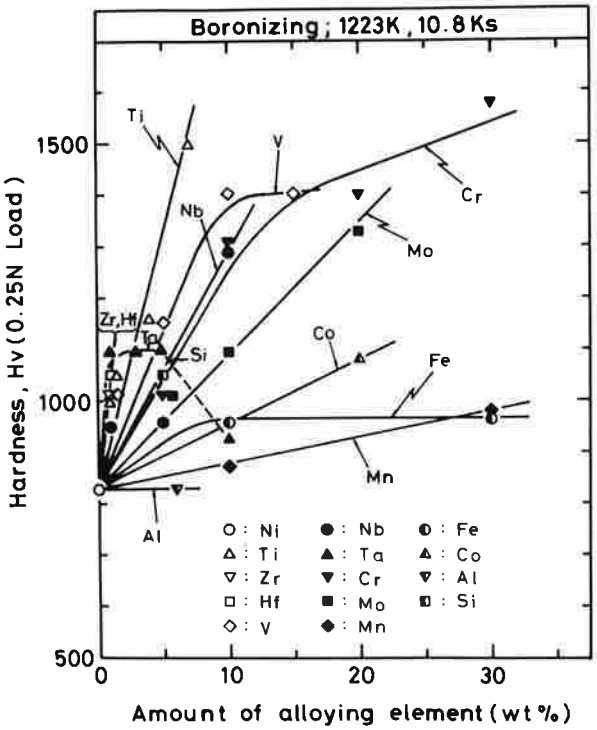

Fig. 27 Effect of individual alloying element on maximum hardness of boride layer in Ni alloy.

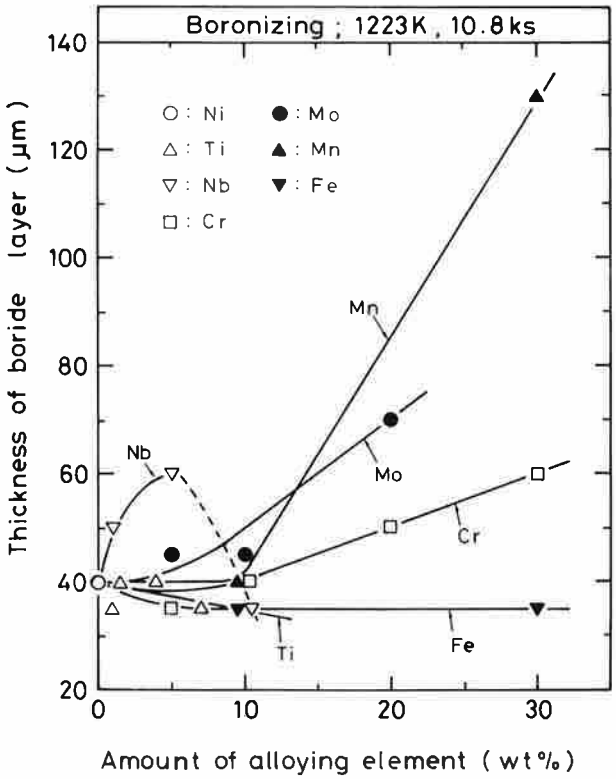

Fig. 28 Effect of individual alloying element on thickness of boride layer in Ni alloy.

Now, if mean of hardness increase per unit alloying element is defined as "hardenability", the decreasing order of hardenability is estimated as IVa group (Ti, Zr, Hf), Va (V, Nb, up to 5 Ta), Si, VIa (Cr, Mo), VIII (Fe, Co) and VIIa (Mn). Moreover Al is no relation to hardenability. Considering amount of solubility in Ni it is concluded that the effective elements for increase in hardness of boronized Ni are Ti, Nb, V, Cr and Mo. In comparison with hardness of boronized Ni the hardness increase in commercial Ni-base alloys is caused due to alloying of the above 5 elements.

Next, **Figure 28** shows the effect of amount of alloying element on thickness of boronized layer which has an apparent increase in hardness compared with base metal. In order to increase the hardened zone compared with Ni, Nb less than 5%, Mn more than 5% and Mo and Cr more than 10% are recommended in Ni alloy. However addition of Ti, Fe and Nb of 10% decreases the thickness of the hardened zone.

(2) X-ray analyses of boride layer

Figure 29 (a) to **(e)** showed the results of X-ray analyses for each alloying group of Ni-binary alloys in comparing with that of Ni after boronizing of 1223K-10.8 Ks. In boronized pure Ni both Ni_2B and Ni_3B were clearly observed. Relative intensity of Ni_2B which was formed at the surface was stronger than that of Ni_3B of the inside. In (a) of 7 Ti, 1 Zr and 1 Hf both Ni_2B and Ni_3B were only formed but no other any alloy boride. However Ni_2B and Ni_3B in Ni-binary alloy were formed in lower 2θ a little. This means, as described in the latter, that some complex Ni_2B and Ni_3B including alloying element are formed in these alloys. In (b) of 5 and 30 Cr both Ni_2B and Ni_3B were formed, but no any Cr boride. In (c) of 5 and 20 Mo both Ni_2B and Ni_3B and MoB were obviously formed. Moreover the other phase unidentified was seen in Ni-Mo alloys. In (d) of 10 and 30 Fe both Ni_2B and Ni_3B were only formed. On (e) of 10 Nb, 6 Al, and 5 Si both Ni_2B and Ni_3B were formed, and some phase unidentified was seen in 10 Nb and 6 Al alloys. Conclusively from X-ray investigation both Ni_2B and Ni_3B which were little transfered to lower 2θ were only formed for boronized Ni-binary alloys up to 30% except Ni-Mo alloy. The increase in hardness of boronized layer by alloying element is estimated to be caused by forming some complex $(Ni, X)_2B$ and $(Ni, X)_3B$ phases, where X is alloying element. Additionally **Fig. 30 (a)** and **(b)** show an example of X-ray images of B, Fe, Ni and line analyses of Ni, Fe, B, O, N, C in XMA for boronized Ni-10Fe alloy. Obvious concentration of Fe was seen for the outside of the boronized layer, that is base alloy side, in both figures. This means that in forming Ni_3B layer, Fe is considerably exclusive. Therefore it is estimated that formation rate of Ni_3B layer is lowered and has a preferred orientation which results in formation of (C) zone. However, as shown Fig. 30 (b) Fe is considerably included in Ni_2B

layer at surface. As described in Fig. 29 (d) there is no formation of Fe boride in X-ray analyses. Judging from these results it is considered that formation of some (Ni, Fe)$_2$B boride increases the hardness of Ni_2B boride layer in Ni metal by solution or fine precipitation hardening mechanism.

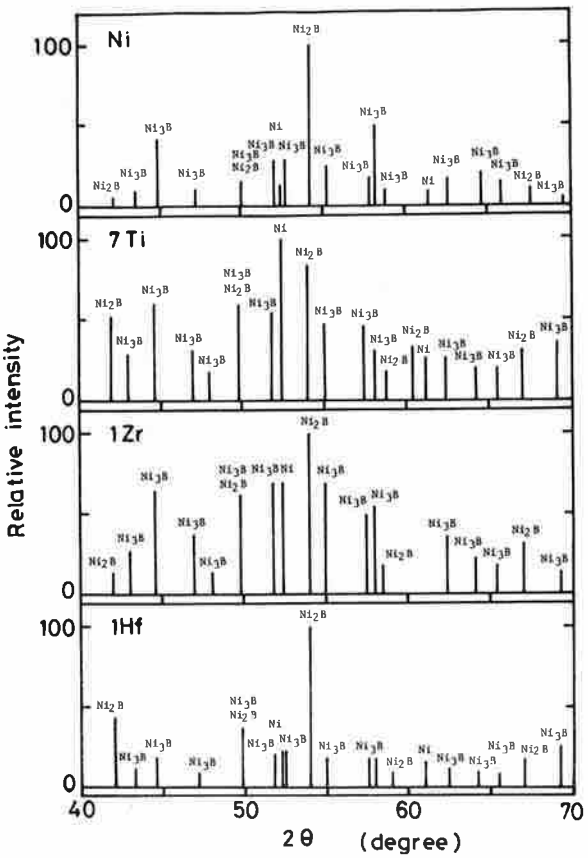

(a) Ni, Ni-Ti, Ni-Zr and Ni-Hf alloys

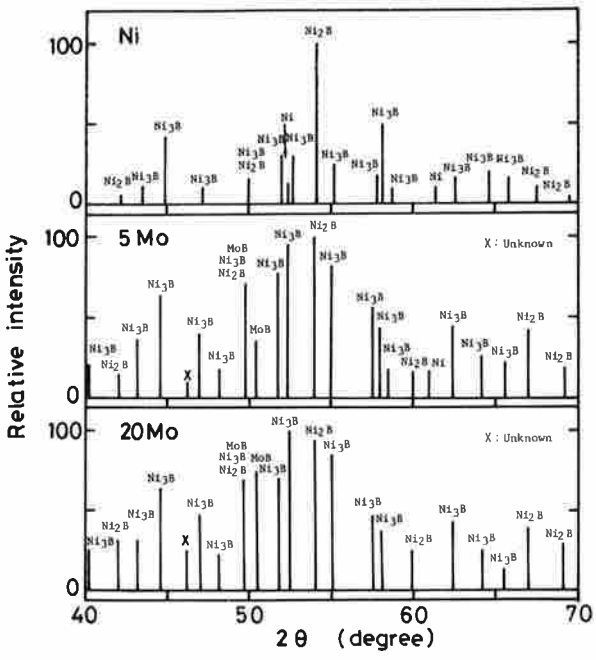

(c) Ni-Mo alloys

3.3 Prediction for Maximum Hardness of Boronized Layer for Ni-base Multialloy

The authors tried to estimate the maximum hardness of boronized layer for Ni-base multialloy by using the simple addition of the hardenability of Ni-binary alloys.

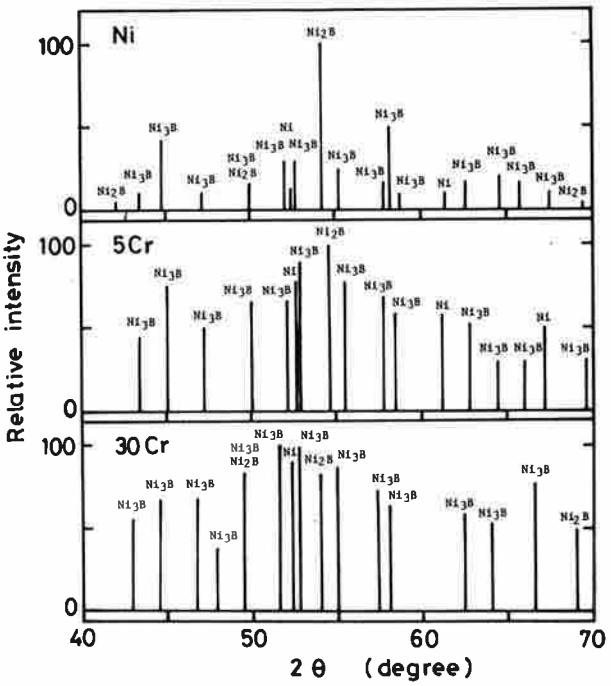

(b) Ni-Cr alloys

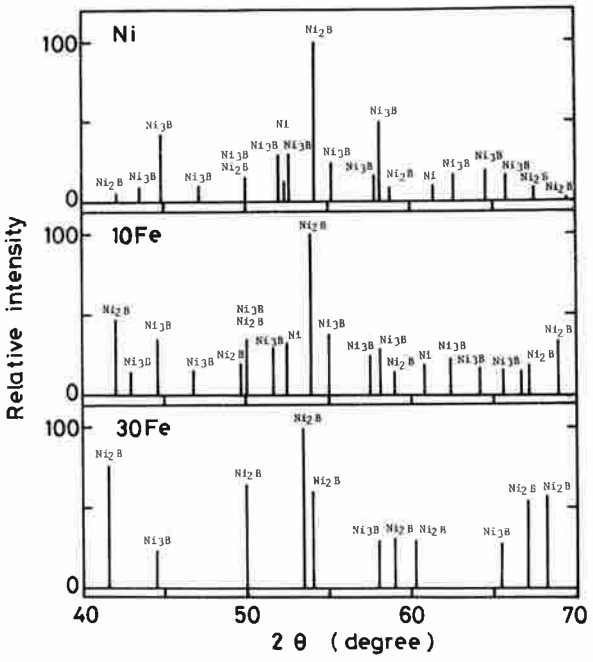

(d) Ni-Fe alloys

Fig. 29 X-ray analyses of boride layer for Ni-binary alloys.
(continue to next page)

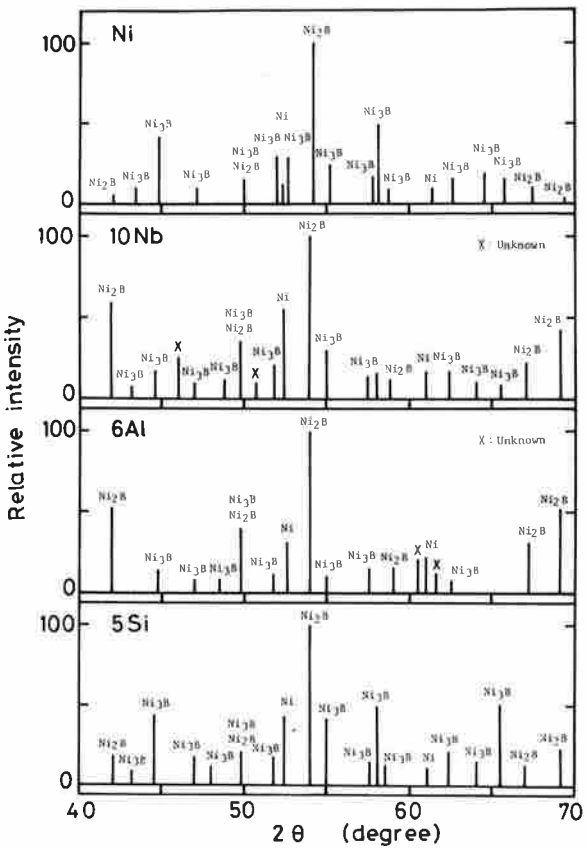

(e) Ni-Nb, Ni-Al and Ni-Si alloys

Using the hardenability of Ni-binary alloys shown in Fig. 27, a predictable equation is introduced as a simple expression. As a result the following equation is given

$$(Hv)c = 220 \cdot Hf\,(wt\%) + 170 \cdot Zr + 95 \cdot Ti + 54 \cdot Ta$$
$$46 \cdot Nb + 44 \cdot Si + 38 \cdot V + 25 \cdot Mo + 13 \cdot Co$$
$$+ 5 \cdot Mn + X_{Cr} + Y_{Fe} + 800 \qquad (1)$$

where, (Hv)c : Vickers hardness calculated of boronized layer after boronizing at 1223K-10.8Ks

X_{Cr} : 47 Cr (Cr $\leqslant$ 10%), 14Cr + 330 (Cr $>$ 10%)

Y_{Fe} : 13 Fe (Fe $\leqslant$ 10%), 130 (Fe $>$ 10%)

For commercial Ni-base alloys shown in Fig. 4 the relation between hardness calculated (Hv)c and measured (Hv)m was shown in **Fig. 31.** However there is some different between them. Roughly the following relation is given

$$(Hv)m = (Hv)c - 430\ (\pm 180) \qquad (2)$$

The hardness measured is 430 (in Hv) less than the hardness calculated in eq. (1).

This difference is considered that some selected alloying elements which are easy to combine with boron preferably forms their borides and the other elements does not form or are not effective to form their borides when

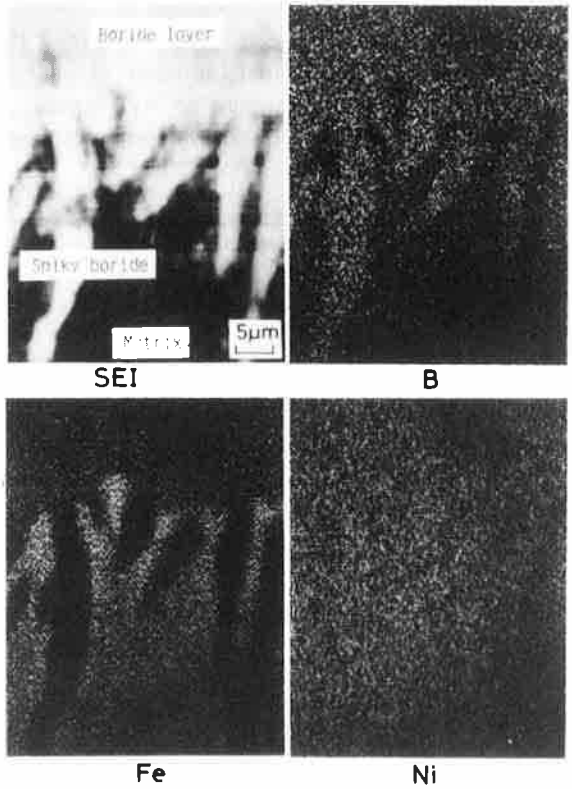

(a) Image patterns of B, Fe and Ni elements

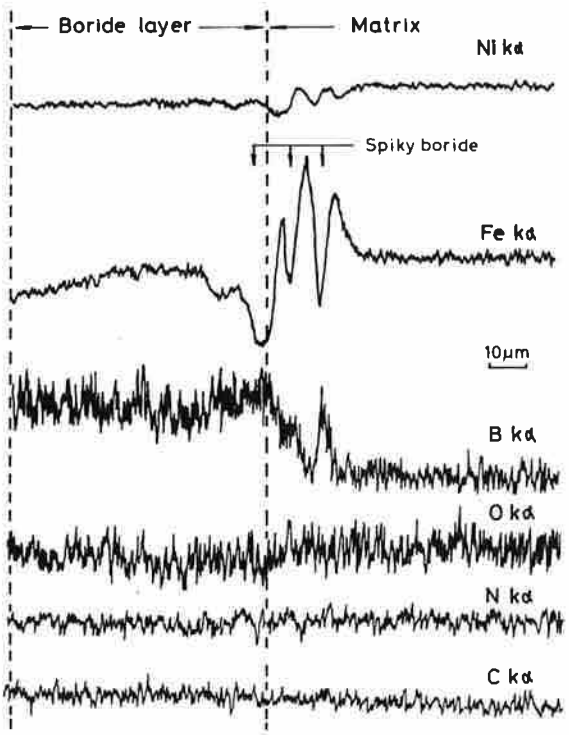

(b) Line analyses of Ni, Fe, B, O, N and C elements

Fig. 30 XMA analyses of boride layer and its boundary of Ni-10 Fe alloy.

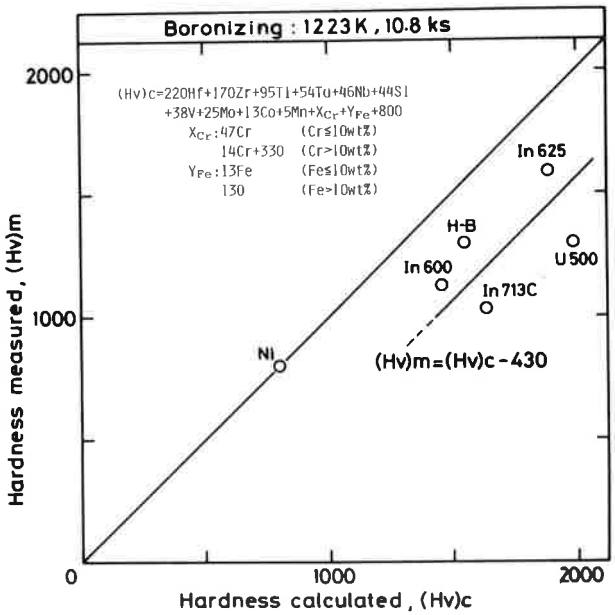

Fig. 31 Relation between maximum hardness of boride layer measured and calculated by hardenability indices in boronized Ni-binary alloys

boronizing is applied. According to investigation of free energy for boride formation, the order of boride formation is estimated to be elements in Group IVa, Group Va and Group VIa, and these elements are much easier in boride formation than Ni. Therefore at the present it is difficult to estimate the boronized hardness of Ni-base multialloy by a simple estimation as eq. (1).

4. Conclusions

The hardnesses and features of boronized layer in 1223K-10.8Ks for commercial Ni-base and experimental Ni-binary alloys have been investigated. The conclusions obtained are as follows;

(1) The hardness of boronized layer of commercial Ni-base alloys showed much higher than that of Ni metal, and reached to Hv 1580 for Inconel 625, Hv 1300 for Udimet 500 and Hastelloy B, Hv 1100 for Inconel 600 and Hv 1040 for Inconel 713C comparing with Hv 800 for Ni metal.
The features of boronized zone of the Ni-base alloys were roughly composed of three different layers as a compound layer, a boride dispersed layer in grain and a boride precipitated zone along grain boundary comparing with single compound layer for Ni metal. The use of boronizing process for Inconel 625 and Hastelloy B is expected for industrial use in the future from the sandpoints of hardness and depth of hardened zone.

(2) As a result of boronizing investigation for experimental Ni-binary alloys, the most effective elements for increasing of hardness are Ti, Zr, Hf of IVa group, and the following elements are V, Nb, Ta of Va group, Cr, Mo of VIa group and Si of IVb group. Fe, Co of VIII group and Mn of VIIb group show a small effect for the increase, but Al does not show.
Therefore the addition of alloying elements of IVa, Va and VIa groups is effective for increasing of hardness for boronized Ni surface. However, considering the limit of these elements for solid solution in Ni metal, the most effective elements are predicted to be Ti, V, Nb, Cr and Mo in case of Ni.

(3) In order to have a hard boronized surface more than Hv 1200 (1.5x boronized hardness of Ni), more than 7% of Ti, 10% of V, Nb or Cr, or 20% of Mo are required in Ni alloy.

(4) From the result of X-ray analyses the layers of Ni_2B and Ni_3B are formed for boronized surface of most Ni-binary alloys less than 30% containing, while Mo boride is formed in case of Ni-Mo alloys.
Therefore, it is considered that such high hardness of boronized surface of Ni-binary alloys causes mainly due to substitution $(Ni, X)_2B$ and $(Ni, X)_3B$ for Ni_2B and Ni_3B, where X is alloying element.

(5) The maximum hardness of boronized commercial Ni-base alloys could not be explained by means of a simple estimation with hardenability of Ni-binary alloys. This is considered that preferable boride formation phenomena occurs among alloying elements in Ni-base multialloys.

Acknowledgement

The authors would like to express their thanks to Mr. Sigeru Kiya, Naoetsu Works, Nippon Stainless Steel Co., Ltd. for his co-operation on making tentative Ni-binary alloys.

References

1) F. Matsuda, K. Nakata et al.: "Surface Hardening of Gold with Boronizing Technique", Proceedings of the Eighth International Precious Metals Institute Conference, 1984, Toronto, Canada, P. 131–145.

2) F. Matsuda and K. Nakata: "Surface Boronizing of Metals and Alloys", Proceedings of the First International Coneference on Surface Engineering, June 1985, Brighton, England, The Surface Engineering Society, P56-1 – P56-12.

3) E. T. Turkdogan: "Physical Chemistry of High Temperature Technology", 1980, Academic Press.

4) S. Ohmori et al.: J. High Temperature Soc. (in Japanese), 8 (1982) 6, 221–229.